Search for Neutralinos and Sleptons in scenarios with Gravitino LSP and Sleptons NLSP with the DELPHI detector up to 202 GeV centre-of-mass energy

R. Alemany[1], F.R. Cavallo[2], C. García[3], F.L. Navarria[2], G. Wolf[1]

Abstract

Sleptons and neutralinos were searched for in the context of scenarios where the lightest supersymmetric particle is the gravitino. It was assumed that the sleptons are the next-to-lightest supersymmetric particles. Data collected with the DELPHI detector at centre-of-mass energies of 192, 196, 200 and 202 GeV were analysed combining the methods developed in previous searches at lower energies. No evidence for the production of these supersymmetric particles was found. Hence, limits were derived at 95% confidence level.

Contributed Paper for ICHEP2000

[1]CERN, CH-1211 Geneva 23, Switzerland
[2]INFN, Bologna, V. le Berti Pichat 6/2, I00126 Bologna, Italy
[3]IFIC, Avda. Dr. Molliner 50, Burjassot 46100, Valencia, Spain

1   Introduction

Supersymmetry (SUSY) may be broken at a scale below the grand-unification scale M_{GUT}, with the ordinary gauge interactions acting as the messengers of supersymmetry breaking [1, 2]. In the corresponding models (GMSB models), the gravitino, $\tilde{G}$, turns out to be the lightest supersymmetric particle (LSP) and is expected to be almost massless. The next-to-lightest supersymmetric particle (NLSP) is therefore unstable and decays, under the assumption of R-parity conservation, into its ordinary matter partner and an invisible gravitino.

The number of generations of supersymmetry breaking messengers and the value of $\tan\beta$ usually determine which supersymmetric particle is the NLSP [3, 4, 5, 6]. In the majority of the GMSB space, the NLSP is a slepton, $\tilde{l}$. Moreover, depending on magnitude of the mixing between $\tilde{\tau}_R$ and $\tilde{\tau}_L$, there exist two possible scenarios. If the mixing is large [4], $\tilde{\tau}_1$ is the NLSP, but if the mixing is negligible, $\tilde{\tau}_1$ is mainly right-handed [7] and almost mass degenerate with the other sleptons. In this case, the $\tilde{e}_R$ and $\tilde{\mu}_R$ three body decay ($\tilde{l} \to \tilde{\tau}_1 \tau l$ with $\tilde{\tau}_1 \to \tau \tilde{G}$), is very suppressed, and $\tilde{e}_R$ and $\tilde{\mu}_R$ decay directly into $l\tilde{G}$. This scenario is called $\tilde{l}$ co-NLSP. Searches for supersymmetric particles within both these scenarios are described in this article.

Due to the coupling of the NLSP to $\tilde{G}$, its mean decay length can range from μm to meters depending on the mass of the gravitino ($m_{\tilde{G}}$):

$$L = 1.76 \times 10^{-3} \sqrt{\left(\frac{E_{\tilde{l}}}{m_{\tilde{l}}}\right)^2 - 1} \left(\frac{m_{\tilde{l}}}{100\,\mathrm{GeV/c^2}}\right)^{-5} \left(\frac{m_{\tilde{G}}}{1\,\mathrm{eV/c^2}}\right)^2 \quad cm \qquad (1)$$

For example, for $m_{\tilde{G}} \lesssim 250$ eV, or equivalently, for a SUSY breaking scale of $\sqrt{F} \lesssim 1000$ TeV (since both parameters are related), the decay of the NLSP can take place within the detector. This range of $\sqrt{F}$ is in fact consistent with astrophysical and cosmological considerations [8, 9].

The results of two searches are presented in this work. The first one looks for the production of $\tilde{\chi}_1^0$ pairs with either $\tilde{\chi}_1^0$ decaying to $\tilde{\tau}_1 \tau$ and $\tilde{\tau}_1$ then decaying promptly into $\tau\tilde{G}$, which is an update of the search presented in ref. [11], or $\tilde{\chi}_1^0$ decaying to $\tilde{l}l$ with $\mathrm{BR}(\tilde{\chi}_1^0 \to \tilde{l}l) = 1/3$ and $\tilde{l}$ promptly decaying into $l\tilde{G}$: $e^+e^- \to \tilde{\chi}_1^0\tilde{\chi}_1^0 \to \tilde{l}l\tilde{l}'l' \to l\tilde{G}ll'\tilde{G}l'$. These two modes represent the two extremes in the range of possible decays of the neutralino. In particular, a higgsino-like $\tilde{\chi}_1^0$ would decay only to $\tilde{\tau}_1 \tau$ for all practical purposes since the higgsino component of the $\tilde{\chi}_1^0$ couples to $\tilde{l}$ through Yukawa couplings. On the other hand, the decays of a gaugino-like $\tilde{\chi}_1^0$ are regulated only by phase space considerations. Therefore, in the case of the $\tilde{\tau}_1$-NLSP scenario, neutralino pair production would mainly lead to a final state with four tau leptons and two gravitinos, while in the case of a co-NLSP scenario, the final signature would contain two pairs of leptons with possibly different flavour and two gravitinos.

The second search concerns $\tilde{l}$ pair production followed by the decays $\tilde{l} \to l\tilde{G}$ within the detector volume. The signature of such an event will be at least one track of a charged particle with a kink or a decay vertex when the $\tilde{l}$ decays inside the tracking devices. If the decay length is too short (small $m_{\tilde{G}}$) to allow for the reconstruction of the $\tilde{l}$ track, only the corresponding lepton or its decay products will be seen in the detector, and the search will then be based on track impact parameter. However, if the decay takes place

---

[4]In GMSB models large mixing occurs generally in regions of $\tan\beta \geq 10$ or $|\mu| > 500$ GeV.

outside the tracking devices (large $m_{\tilde{G}}$), the signature will be that of a heavy charged particle already studied by DELPHI [12]. For very light gravitinos the limits from the search for sleptons in gravity mediated (MSUGRA) models can be applied [13, 14].

The data samples and event selections are respectively described in sections 2 and 3, while the results and a model dependent interpretation are presented in section 4.

2   Event sample and experimental procedure

All searches are based on data collected with the DELPHI detector during 1999 at the centre-of-mass energies of 192, 196, 200 and 202 GeV. The total integrated luminosity was 228.2 pb^{-1}. A detailed description of the DELPHI detector can be found in [16] and its performance in [17]. In all cases, the $\tilde{\tau}_1$ and $\tilde{l}$ searches are updates to similar searches carried out at lower centre-of-mass energies.

To evaluate the signal efficiencies and background contaminations, events were generated using different programs, all relying on JETSET 7.4 [18], tuned to LEP 1 data [19] for quark fragmentation. The program SUSYGEN [20] was used to generate the neutralino pair events and their subsequent decay products. In order to compute detection efficiencies, a total of 90000 events were generated with masses 67 GeV/$c^2 \leq m_{\tilde{\tau}_1} + 2$ GeV/$c^2 \leq m_{\tilde{\chi}_1^0} \leq \sqrt{s}/2$. Slepton pair samples of 99000 and 76500 events at 196 GeV and 202 GeV respectively were produced with PYTHIA 5.7 [18] with staus having mean decay lengths from 0.25 to 200 cm and masses from m_τ to 98 GeV/c^2. Another sample of $\tilde{\tau}$ pair was produced with SUSYGEN for the small impact parameter search with $m_{\tilde{\tau}}$ from 40 to 80 GeV/c^2.

The background process e$^+$e$^- \to q\bar{q}(n\gamma)$ was generated with PYTHIA 6.125, while KORALZ 4.2 [21] were used for $\mu^+\mu^-(\gamma)$ and $\tau^+\tau^-(\gamma)$. The generator BHWIDE [22] was used for e$^+$e$^- \to$ e$^+$e$^-$ events.

Processes leading to four-fermion final states, were generated using EXCALIBUR 1.08 [23] and GRC4F [24].

Two-photon interactions leading to hadronic final states were generated using TWOGAM [25], separating the VDM, QPM and QCD components. The generators of Berends, Daverveldt and Kleiss [26] were used for the leptonic final states.

The cosmic radiation background was studied using the data collected before the beginning of the 1998 LEP run.

The generated signal and background events were passed through the detailed simulation [17] of the DELPHI detector and then processed with the same reconstruction and analysis programs used for real data.

3   Data selection

3.1   Neutralino pair production

The selection used in the search for the process e$^+$e$^- \to \tilde{\chi}_1^0\tilde{\chi}_1^0 \to \tilde{\tau}_1\tau\tilde{\tau}_1\tau \to \tau\tilde{G}\tau\tau\tilde{G}\tau$ has been described in [10, 11]. A very similar selection was used in the general search for e$^+$e$^- \to \tilde{\chi}_1^0\tilde{\chi}_1^0 \to \tilde{l}l\tilde{l}'l' \to l\tilde{G}ll'\tilde{G}l'$ within the co-NLSP scenario, where BR$(\tilde{\chi}_1^0 \to \tilde{l}l) = 1/3$ for each leptonic flavour. The main two differences between these two cases comes from the fact that the mean number of neutrinos carrying away undetected energy and

2

momentum and the number of charged tracks per event is considerably bigger for the $\tilde{\tau}_1$-NLSP scenario.

The pre-selection of events is common to both scenarios, and has been described in [10], together with the selection of $\tilde{\chi}_1^0 \to \tilde{\tau}_1\tau$ channel. Only the details of the search $\tilde{\chi}_1^0 \to \tilde{l}l$ are presented in the following. Two sets of cuts were applied in order to reduce the $\gamma\gamma$ and $f\bar{f}(\gamma)$ backgrounds and a third set of cuts to select events according to their topology:

1- Cuts against $\gamma\gamma$ backgrounds: the transverse energy, E_T, should be bigger than 4 GeV. The energy in a cone of 30° around the beam axis was further restricted to be less than 60% of the total visible energy to avoid possible bias from the Monte Carlo samples. The missing mass should be smaller than $0.88\sqrt{s}$. The momentum of the charged particle with largest momentum should be bigger than 8 GeV/c. The transverse missing momentum, p_T, should be bigger than 6 GeV/c. These cuts reduced the $\gamma\gamma$ background by a factor of the order of 40.

2- Cuts against $f\bar{f}(\gamma)$ and 4-fermion backgrounds: the number of good tracks should be smaller than 7. The maximum thrust was further reduced from 0.99 to 0.95. Dividing each event into two jets with the Durham algorithm, its acoplanarity should be bigger than 8°. The missing mass of the events should be bigger than $0.2\sqrt{s}$. After these cuts, the $f\bar{f}(\gamma)$ and 4-fermion backgrounds were reduced by a factor of the order of 30.

3- Cuts based on topology: signal events tend naturally to cluster into a 4-jet topology. When events are forced into a 4-jet configuration, all jets should be at least 18° away from the beam direction. When reduced by the jet algorithm into a 2-jet configuration, the charged particles belonging to each of these jets should be in a cone broader than 25°. Finally, the axes of each of the four jets should be separated from the others at least by 9°.

6 events were observed to pass the search for neutralino pair production in the $\tilde{\tau}_1$-NLSP scenario, with 3.36±0.98 SM background events expected. 4 events pass the search for neutralino pair production in the co-NLSP scenario, with 4.39±0.51 SM background events expected. After these cuts, efficiencies between 20 and 44% were obtained for the signal events.

3.2   Slepton pair production

This section describes the update of the search for the process $e^+e^- \to \tilde{\tau}\tilde{\tau} \to \tau\tilde{G}\tau\tilde{G}$ already described in [10, 27, 11]. An additional 228.2 pb^{-1} integrated luminosity collected at the centre-of-mass energies of 192, 196, 200 and 202 GeV has been analysed using the same procedure as for the data collected at 189 GeV, and using the same values for the data selection cuts taking into account the necessary rescaling of some cuts with the energy. The same selection cuts have been applied to the search for $\tilde{\mu}_R$- pair production in the framework of $\tilde{l}$ co-NLSP scenario. Therefore, only results and efficiencies will be reported in this section, since the details of the selection criteria can be found in [10, 27, 11].

3.2.1 Search for secondary vertices

This analysis exploits a peculiarity of the $\tilde{l} \to l\tilde{G}$ topology in the case of intermediate gravitino masses (i.e. $0.5\ \text{eV}/c^2 \lesssim m_{\tilde{G}} \lesssim 200\ \text{eV}/c^2$ as dictated by eq. 1), namely, one or two tracks coming from the interaction point and at least one of them with either a secondary vertex or a kink.

Rather loose preselection cuts were imposed on the events in order to suppress the low energy background (beam-gas, beam-wall, etc), $\gamma\gamma$, e^+e^- and hadronic events. The events that survived the preselection cuts underwent the search for secondary vertices or kinks.

Fake decay vertices could be present amongst the reconstructed secondary vertices, being produced by particles interacting in the detector material or by radiated photons if the particle trajectory was reconstructed into two separated tracks. To eliminate these classes of events, additional requirements were imposed:

- to reject hadronic interactions, the angle between the direction of any reconstracted hadronic vertex (secondary vertices reconstructed in region where there is material), and the direction of the slepton candidate must be greater than 5°;

- to reject segmented tracks, the angle between the tracks used to define a vertex had to be larger than 6°;

- to reject photon radiation in the case of τ clusters with only one track, there had to be no neutral particle in a 3° cone around the direction defined by the difference between the $\tilde{\tau}_1$ momentum and the momentum of the τ daughter calculated at the crossing point.

If no pair of tracks was found to survive these conditions, the event was rejected. Figure 1 shows the distribution of these three quantities. The distributions compare real data, expected Standard Model background simulation and simulated signal for $m_{\tilde{\tau}_1} = 60\ \text{GeV}/c^2$ decaying with a mean decay length of 50 cm. All the samples are at 200 GeV centre-of-mass energy. The excess of data in the first bins of fig. 1-b is due to an underestimation in the simulation of mismatchings between the tracking devices.

Two events in real data were found to satisfy all the conditions described above, while $0.79^{+0.28}_{-0.12}$ were expected from SM backgrounds. One event was compatible with a $\gamma\gamma \to \tau^+\tau^-$ with a hadronic interaction in the ID detector. The other one was compatible with a $e^+e^- \to \tau^+\tau^-$ event where one of the electrons (decay product of the τ), after radiating a photon, was reconstructed as two independent tracks.

The vertex reconstruction procedure was sensitive to radial decay lengths, R, between 20 cm and 90 cm. Within this region a vertex was reconstructed with an efficiency of 54.0±2.0%. The VD (Vertex Detector) and the ID (Inner Detector) were needed to reconstruct the $\tilde{\tau}$ track and the TPC (Time Projection Chamber) to reconstruct the decay products. The shape of the efficiency distribution was essentially flat as a function of R, going down when the $\tilde{\tau}$ decayed near the outer surface of the TPC, due to inefficiencies in the reconstruction of the tracks coming from the desintegration products of the τ.

The search for vertices had an efficiency of 52.8±2.0% for $\tilde{\tau}$ masses between 40 and 98 GeV/c^2 with a mean decay length of 50 cm. The efficiencies decreased near the kinematical limit due to a small boost that allowed for big angles to appear between the

$\tilde{\tau}$ and the desintegration products of the τ. For $\tilde{\tau}$ masses below 40 GeV/c^2, the efficiency decreased gradually due to the cut that rejects segmented tracks. This happened because the resulting big boost causes the angle between $\tilde{\tau}$ and τ decay products to be very small.

As already said, the same selection criteria was applied to smuons. The efficiency for smuons was 56.5±2.0% for $m_{\tilde{\mu}_R}$ between 40 to 98 GeV/c^2.

3.2.2 Large impact parameter search

To investigate the region of lower gravitino masses the previous search was extended to the case of sleptons with mean decay length between 0.25 cm and approximately 10 cm. In this case the $\tilde{l}$ track is not reconstructed and only the l (or the decay products in the case of $\tilde{\tau}$) is detected. The impact parameter search was only applied to those events accepted by the same general requirements as in the search for secondary vertices, and not selected by the vertex analysis. The same selection criteria described in references [10, 27, 11] were applied.

The efficiencies were derived for the different $\tilde{\tau}_1$ masses and decay lengths by applying the same selection to the simulated signal events. The maximum efficiency was 31.0±2.0% corresponding to a mean decay length of 2.5 cm. The efficiency decreased very fast for lower decay lengths due to the cut on minimum impact parameter. For longer decay lengths, the appearance of reconstructed $\tilde{\tau}$ tracks in combination with the cut on the maximum amount of charged particle tracks caused the efficiency to decrease smoothly. This decrease is compensated by a rising efficiency in the search for secondary vertices. For masses above 30 GeV/c^2 no dependence on the $\tilde{\tau}$ mass was found far from the kinematic limit.

The same selection was applied to smuons. For smuons the efficiency increased to 60.0±2.0% for a mean decay length of 2.5 cm and masses over 30 GeV/c^2 since the smuon has always a one-prong decay.

Trigger efficiencies were studied simulating the DELPHI trigger response to the events selected by the vertex search and by the large impact parameter analysis, and were found to be around 99%.

Two events in the real data sample were selected with the above criteria, while $1.77^{+0.25}_{-0.21}$ were expected from SM backgrounds. Both events are compatible with $e^+e^- \rightarrow \tau^+\tau^-$ events where one of the electrons (decay product of the τ), after radiating a photon, was reconstructed as an ID-TPC track giving a very large impact parameter track.

3.2.3 Small impact parameter search

The large impact parameter search can be extended further down to mean decay lengths below 1 mm. Here we recall only the main points of the analysis and some changes with respect to previous ones. In low multiplicity events two hemispheres were defined using the thrust axis. The highest momentum, good quality ($\Delta p/p < 50\%$), tracks in each hemisphere were labelled leading tracks. The impact parameters, b_1 and b_2, of the leading tracks in the Rϕ plane were used to discriminate against SM backgrounds. The same selection criteria described in reference [10, 11] was applied. However, some extra selection was added in order to reduce the background from detector noise or failure.

In order to preserve the efficiency in the region of decay length $\gtrsim 10$ cm, where the $\tilde{\tau}$ can be observed as a track coming from the primary vertex and badly measured owing to its limited length, further requirements on the track quality were applied only to the leading track having the maximum impact parameter. This track was required to have a relative momentum error $< 30\%$ and to be measured in the TPC or in all of the other three track detectors in the barrel.

The efficiency of the search did not show any significant dependence on the $\tilde{\tau}$ mass for masses over 40 GeV/c^2, and it could be parameterized as a function of the $\tilde{\tau}$ decay length in the laboratory system. The maximum efficiency was $\sim 38\%$ for a mean decay length of ~ 2 cm, the efficiency dropped at small decay lengths ($\sim 10\%$ at 0.6 mm).

The same selection criteria were used to search for smuons as reported in [10, 11]. The maximum efficiency reached for the smuon search was 43% at 2 cm of mean decay length.

With $\sqrt{b_1^2 + b_2^2} > 600 \mu$m the number of events selected in the data was 5 for the $\tilde{\tau}$ and $\tilde{\mu}$ search. 5.05$\pm$0.39 events were expected from the Standard Model background. Fig. 2 shows the $\sqrt{b_1^2 + b_2^2}$ distribution for data (dots) and simulated backgrounds (histogram) after all other cuts. All of the selected candidates were compatible with Standard Model events.

4   Results and interpretation

Since no evidence for a signal was found in the data, limits on the cross-section of sparticle pair production and on the masses of the particles searched for were derived. In what follows, the model described in reference [4] will be used in order to derive limits. This is a model which assumes radiatively broken electroweak symmetry and null trilinear couplings at the messenger scale. The corresponding parameter space was scanned as follows: $1 \leq n \leq 4$, 5 TeV $\leq \Lambda \leq$ 90 TeV, $1.1 \leq M/\Lambda \leq 10^9$, $1.1 \leq \tan\beta \leq 50$, and $sign(\mu) = \pm 1$, where n is the number of messenger generations in the model, Λ is the ratio between the vacuum expectation values of the auxiliary component and the scalar component of the superfield and M is the messenger mass scale. The parameters $\tan\beta$ and μ are defined as for MSUGRA.

4.1   Neutralino pair production

Limits on the cross-section for neutralino pair production were derived in the two scenarios for each $(m_{\tilde{\chi}_1^0}, m_{\tilde{l}})$ combination. For the $\tilde{\tau}_1$-NLSP case, the combination took into account the results from the LEP runs from 1996 to 1998 [10, 11]. The limits for the production cross-section allowed us to exclude some sectors of the $(m_{\tilde{\chi}_1^0}, m_{\tilde{l}})$ space. In order to achieve the maximum sensitivity, the results from two other analyses are taken into account. The first is the search for slepton pair production in the context of gravity mediated SUSY breaking models [13, 14]. In the case where the MSUGRA $\tilde{\chi}_1^0$ is massless, the kinematics corresponds to the case of $\tilde{l}$ decaying into a lepton and a gravitino. The second is the search for lightest neutralino pair production in the region of the mass space where $\tilde{\chi}_1^0$ is the NLSP [29, 30] (the region above the diagonal line in fig. 3, i.e. $m_{\tilde{\tau}} > m_{\tilde{\chi}_1^0}$). Within this zone, the neutralino decays into a gravitino and a photon.

As an illustration, fig. 3 presents the 95% C.L. excluded areas for $m_{\tilde{G}} < 1$ eV/c^2

in the $m_{\tilde{\chi}_1^0}$ *vs.* $m_{\tilde{\tau}_R}$ plane for the co-NLSP case. The positive-slope dashed area is excluded by this analysis. The negative-slope dashed area is excluded by the analysis searching for neutralino pair production followed by the decay $\tilde{\chi}_1^0 \to \tilde{G}\gamma$. The point-hatched area is excluded by the direct search for slepton pair production within MSUGRA scenarios [13, 14].

4.2   Slepton pair production

Since there was no evidence for the signal above the expected background, the number of candidates in data and the expected number of background events were used to set upper limits at 95% C.L. for the slepton pair production cross-section and slepton masses. The limits presented here are at $\sqrt{s} = 202$ GeV after combining the results of the searches at $\sqrt{s} = 130\text{-}202$ GeV with the likelihood ratio method [28]. The results are presented in the $(m_{\tilde{G}}, m_{\tilde{l}})$ plane combining the two impact parameter searches, the secondary vertex analysis and the stable heavy lepton search [12].

The $\tilde{\tau}_1$ pair production cross-section depends on the mixing in the stau sector. Therefore, in order to put limits to the $\tilde{\tau}_1$ mass the mixing angle has to be fixed. The results presented here corresponds to the case when there is no mixing between the $\tilde{\tau}_R$ and $\tilde{\tau}_L$, thus $\tilde{\tau}_1$ is a pure right-handed state (figure 4-a). The case which corresponds to a mixing angle which gives the minimum $\tilde{\tau}_1$ pair production cross-section, which at the same time maintains $m_{\tilde{\tau}_1}^2 > 0$, reduces the given limit by 1 GeV. The impact parameter and secondary vertex analyses allow the exclusion of $\tilde{\tau}_R$ with a mass below 88 GeV/c^2 for gravitino masses between 20 and 300 eV/c^2 at 95% C.L.. For $m_{\tilde{G}}$ below a few eV/c^2, $m_{\tilde{\tau}_1} < 75$ GeV/c^2 were excluded by the search for $\tilde{\tau}_1$ in gravity mediated models [14]. For $m_{\tilde{G}}$ larger than 1000 eV/c^2 the limit was 93 GeV/c^2, obtained from the stable heavy lepton search [12].

Within the sleptons co-NLSP scenario, the cross-section limits were used to derive limits for $\tilde{\mu}_R$ (figure 4-b) mass at 95% C.L.. Therefore, within the co-NLSP scenario, the impact parameter search and the secondary vertex search allow for the exclusion of $\tilde{\mu}_R$ masses below 91 GeV/c^2 for gravitino masses between 40 and 200 eV/c^2. For $m_{\tilde{G}}$ below a few eV/c^2, $m_{\tilde{\mu}_R} < 86$ GeV/c^2 were excluded by the search for $\tilde{\mu}_R$ in gravity mediated models [14].

Assuming mass degeneracy between the staus and smuons, (fig. 4-c), these searches exclude at 95% C.L. $\tilde{l}_R$ masses below 93.5 GeV/c^2 for $\tilde{G}$ masses between 30 and 250 eV/c^2. For very short lifetimes only $\tilde{\mu}_R$ was considered since it is the best limit that can be achieved in absence of slepton combination.

For $\tilde{G}$ larger than 1000 eV/c^2 the limit was 93 GeV/c^2, obtained from the stable heavy lepton search [12]. $\tilde{l}_R$ masses below 35 GeV/c^2 are excluded from LEP 1 data [32]. In the case of $\tilde{l}_R$ degeneracy, this limit improves to 41 GeV/c^2.

5   Summary

Lightest neutralino- and slepton-pair production were searched for in the context of light gravitino scenarios. Two scenarios were explored: the $\tilde{\tau}_1$ NLSP and the $\tilde{l}_R$ co-NLSP scenarios. No evidence for signal production was found. Hence, the DELPHI collaboration sets lower limits at 95% C.L. for the mass of the $\tilde{\chi}_1^0$ at 86 GeV/c^2 if $m_{\tilde{G}} \leq 1$ eV/c^2, for

the mass of the $\tilde{\tau}_R$ at 88 GeV/c^2, for the mass of the $\tilde{\mu}_R$ at 91 GeV/c^2, and finally for the mass of the $\tilde{l}_R$ at 93.5 GeV/c^2 for $m_{\tilde{G}}$ in the range between 20 and 300 eV/c^2.

References

[1] M. Dine, W. Fischler and M. Srednicki, Nucl. Phys. **B189** (1981) 575 ;
S. Dimopoulos and S. Raby, Nucl. Phys. **B192** (1981) 353 ;
M. Dine and W. Fischler, Phys. Lett. **B110** (1982) 227 ;
M. Dine and M. Srednicki, Nucl. Phys. **B202** (1982) 238 ;
L. Alvarez-Gaumé, M. Claudson and M. Wise, Nucl. Phys. **B207** (1982) 96 ;
C. Nappi and B. Ovrut, Phys. Lett. **B113** (1982) 175 .

[2] M. Dine and W. Fischler, Nucl. Phys. **B204** (1982) 346 ;
S. Dimopoulos and S. Raby, Nucl. Phys. **B219** (1983) 479.

[3] J. A. Bagger, K. Matchev, D. M. Pierce and R. Zhang, Phys. Rev. **D55** (1997) 3188.

[4] D. A. Dicus, B. Dutta, S. Nandi, Phys. Rev. **D56** (1997) 5748 ;
D. A. Dicus, B. Dutta, S. Nandi, Phys. Rev. Lett. **78** (1997) 3055 ;
K. Cheung, D. A. Dicus, B. Dutta, S. Nandi, Phys. Rev. **D58** (1998) 015008 .

[5] F. Borzumati, *On the Minimal Messenger Model*, hep-ph/9702307 and WIS/96-50-PH, Dec. 1996.

[6] G. F. Giudice, R. Rattazzi, Phys. Rep. 322 (1999) 419..

[7] A. Bartl *et. al.*, Z. Phys. **C73** (1997) 469.

[8] S. Dimopoulos, M. Dine, S. Raby, S. Thomas and J. D. Wells, Nucl. Phys. Proc. Suppl. **A52** (1997) 38.

[9] E. Calzetta, A. Kandus, F. D. Mazzitelli and C. E. M. Wagner, CERN-TH/99-261 and hep-ph/9908524.

[10] DELPHI Collaboration, P. Abreu *et al.*, E. Phys.J. **C7** (1999) 595.

[11] DELPHI Collaboration, P. Abreu *et al.*, CERN-EP/2000-015, Submitted to E. Phys.J.

[12] DELPHI Collaboration, P. Abreu *et al.*, ICHEP2000 Osaka Conference, DELPHI 2000-085 CONF 384.
DELPHI Collaboration, P. Abreu *et al.*, CERN-EP-2000-020 submitted to Phys. Lett. **B**.
DELPHI Collaboration, P. Abreu *et al.*, Phys. Lett. **B444** (1998) 491;

[13] DELPHI Collaboration, P. Abreu *et al.*, "Searches for sleptons at $\sqrt{s} = 183$ and 189 GeV", to be submitted to Phys. Lett. **B**.

[14] DELPHI Collaboration, P. Abreu *et al.*, ICHEP2000 Osaka Conference, DELPHI 2000-093 CONF 392.

[15] DELPHI Collaboration, P. Abreu *et al.*, Phys. Lett. **B466** (1999) 61.

[16] DELPHI Collaboration, P. Aarnio *et al.*, Nucl. Instr. and Meth. **303** (1991) 233.

[17] DELPHI Collaboration, P. Abreu *et al.*, Nucl. Instr. and Meth. **378** (1996) 57.

[18] T. Sjöstrand, Comp. Phys. Comm. **39** (1986) 347;
T. Sjöstrand, `PYTHIA 5.6` *and* `JETSET 7.3`, CERN-TH/6488-92.

[19] DELPHI Collaboration, P. Abreu *et al.*, Z. Phys. **C73** (1996) 11.

[20] SUSYGEN 2.20, S. Katsanevas and S. Melachroinos in *Physics at LEP2*, CERN 96-01, Vol. 2, p. 328 and http://lyoinfo.in2p3.fr/susygen/susygen.html ;
S. Katsanevas and P. Moravitz, Comp. Phys. Com. 122 (1998) 227.

[21] S. Jadach, B.F.L. Ward and Z. Was, Comp. Phys. Comm. **79** (1994) 503.

[22] S. Jadach, W. Placzek, B.F.L. Ward, Comp. Phys. Comm. **79** (1994) 503.

[23] F.A. Berends, R. Pittau, R. Kleiss, Phys. Lett. **B390** (1997) 298.

[24] J. Fujimoto *et al.*, Comp. Phys. Comm. **100** (1997) 128.

[25] S. Nova, A. Olshevski, and T. Todorov, *A Monte Carlo event generator for two photon physics*, DELPHI note 90-35 (1990).

[26] F.A. Berends, P.H. Daverveldt, R. Kleiss, Comp. Phys. Comm. **40** (1986) 271, Comp. Phys. Comm. **40** (1986) 285, Comp. Phys. Comm. **40** (1986) 309.

[27] DELPHI Collaboration, P. Abreu *et al.*, Eur. Phys. J. **C6** (1999) 385.

[28] A.L. Read, *Optimal statistical analysis of search results based on the likelihood ratio and its application to the search for the MSM Higgs boson at* $\sqrt{s} = 161$ *and* 172 *GeV*, DELPHI 97-158 PHYS 737 (1997) and references therein.

[29] DELPHI Collaboration, P. Abreu *et al.*, Eur. Phys. J.**C6** (1999) 371;
DELPHI Collaboration, P. Abreu *et al.*, "Photons events with missing energy at LEP 2", CERN-EP-2000-021, submitted to Eur. Phys. J. **C**.

[30] DELPHI Collaboration, P. Abreu *et al.*, DELPHI 2000-020 CONF 341.

[31] JADE Collaboration, W. Bartel *et al.*, Phys. Lett. B152 (1985) 392.

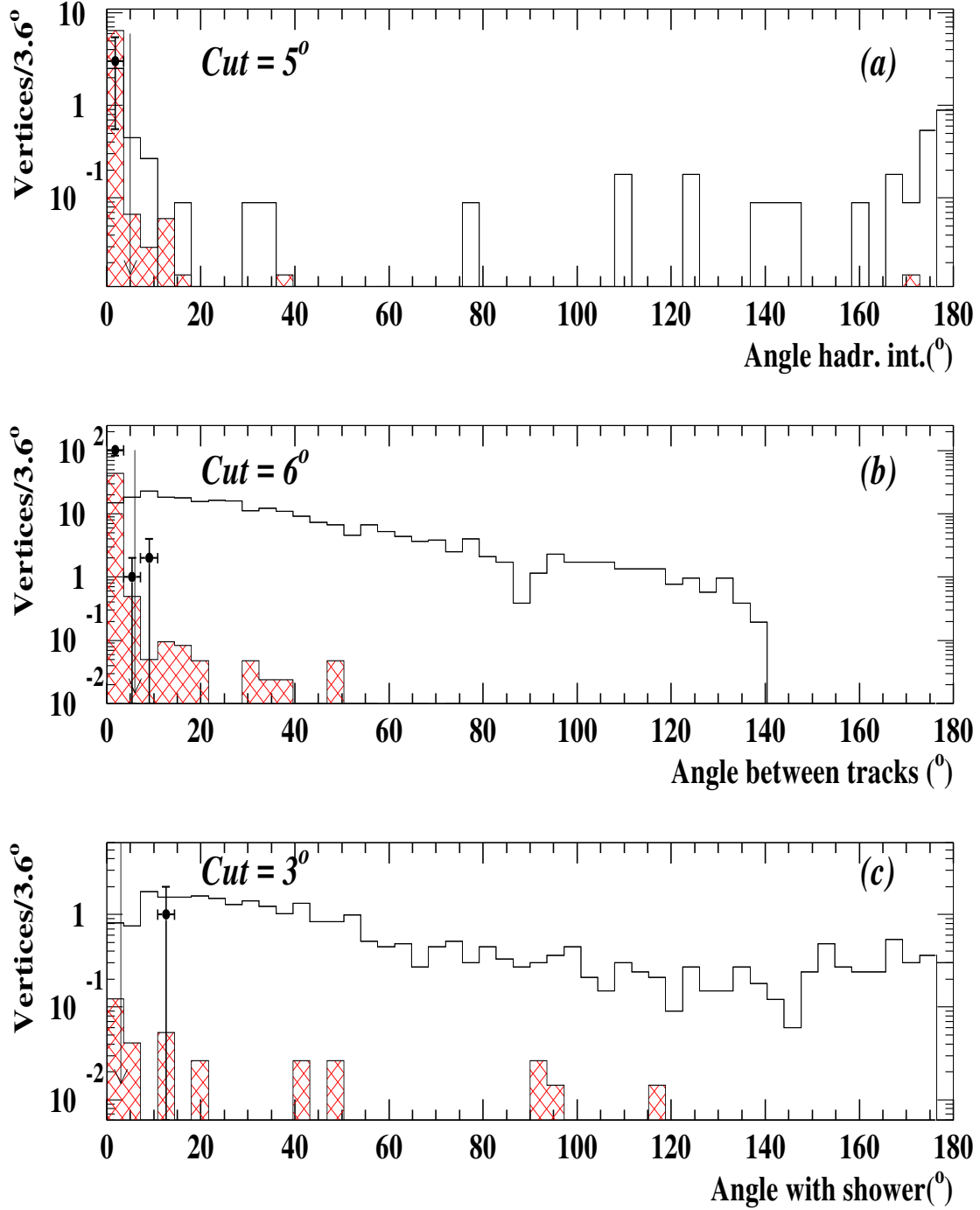[32] Particle Data Group, Eur. Phys. J. **C3** (1998) 1.

Figure 1: (a) Angle between the directions defined by the hadronic vertex and the reconstructed vertex, (b) angle between the tracks of the kink, and (c) angle between the electromagnetic shower and the direction defined by the difference between the momenta of the $\tilde{\tau}_1$ and its associated τ, defined at the crossing point for real data (dots), expected Standard Model background (cross-hatched histogram) and simulated signal for $m_{\tilde{\tau}_1} = 60$ GeV/c^2 decaying with a mean distance of 50 cm (blank histogram). Events that do not have hadronic interactions are not included in (a), and events without electromagnetic showers are not included in (b). All the samples are at 200 GeV centre-of-mass energy. The arrows indicate the selection criteria imposed.
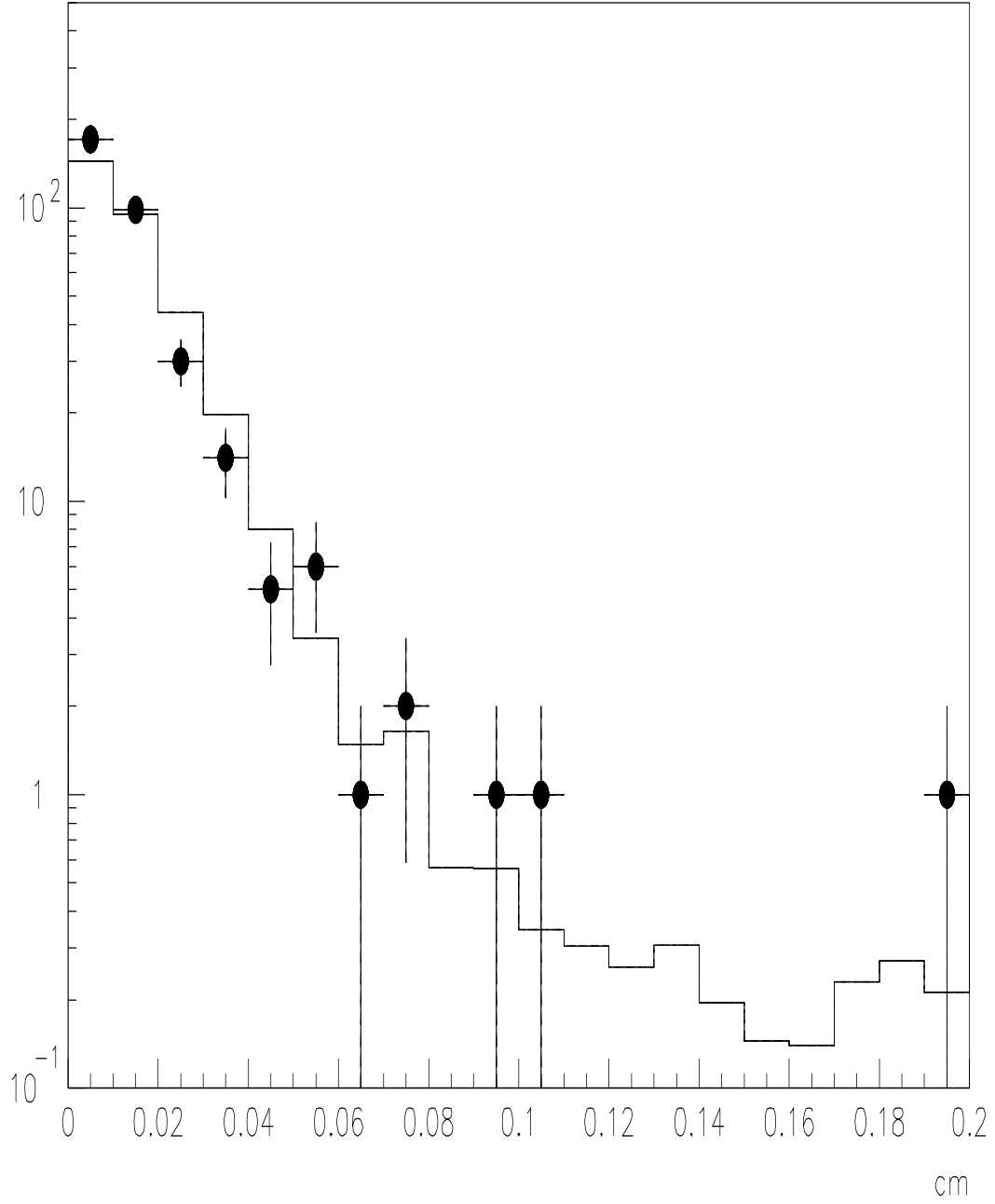
11

Figure 2: $\sqrt{b_1^2 + b_2^2}$ distribution for data (dots) and simulated backgrounds (histogram) after all other cuts applied by the small impact parameter search.
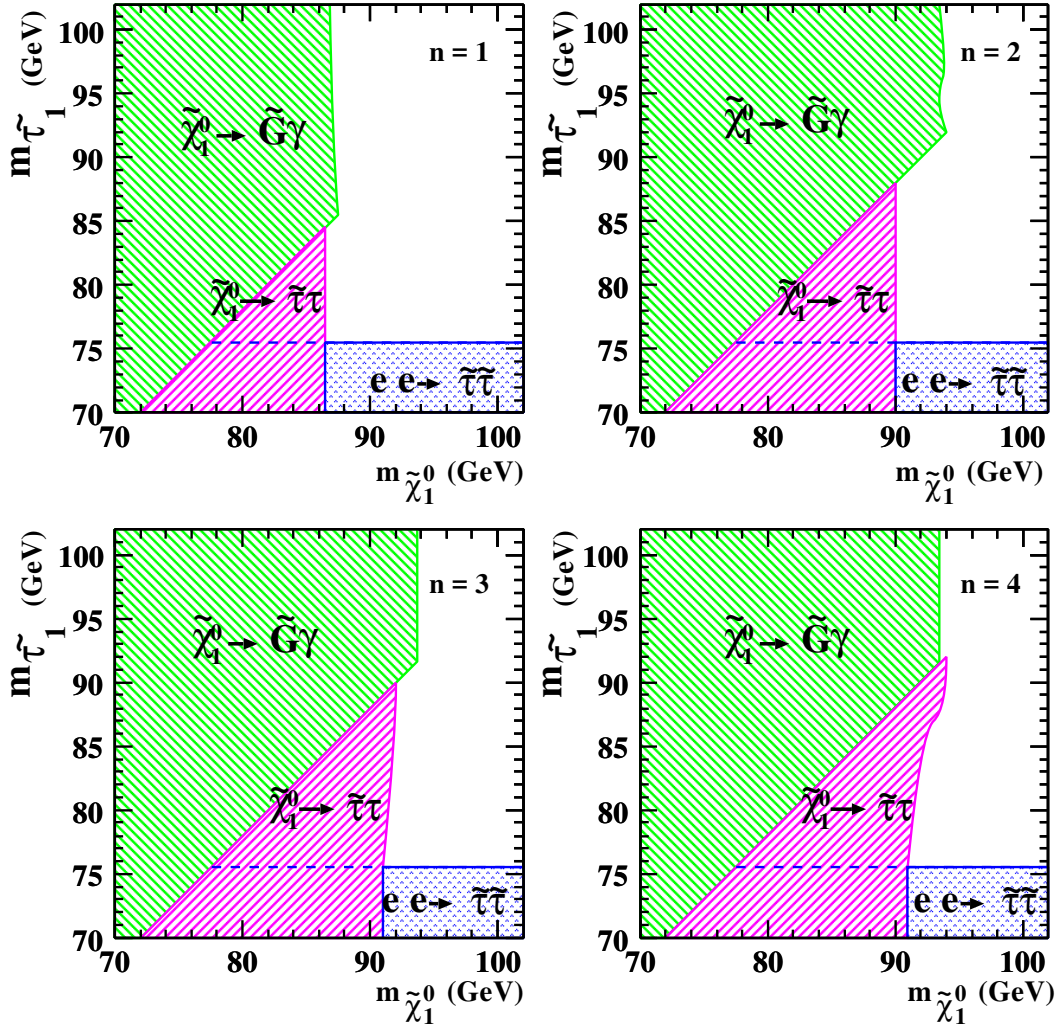
Figure 3: Areas excluded at 95% C.L. with $m_{\tilde{G}} < 1$ eV/c^2 in the $m_{\tilde{\chi}_1^0}$ vs. $m_{\tilde{\tau}_R}$ plane for $n = 1$ to 4. The positive-slope dashed area is excluded by this analysis. The negative-slope dashed area is excluded by the search for $\tilde{\chi}_1^0 \to \gamma\tilde{G}$, and the point-hatched area by the direct search for stau pair production in the MSUGRA framework.
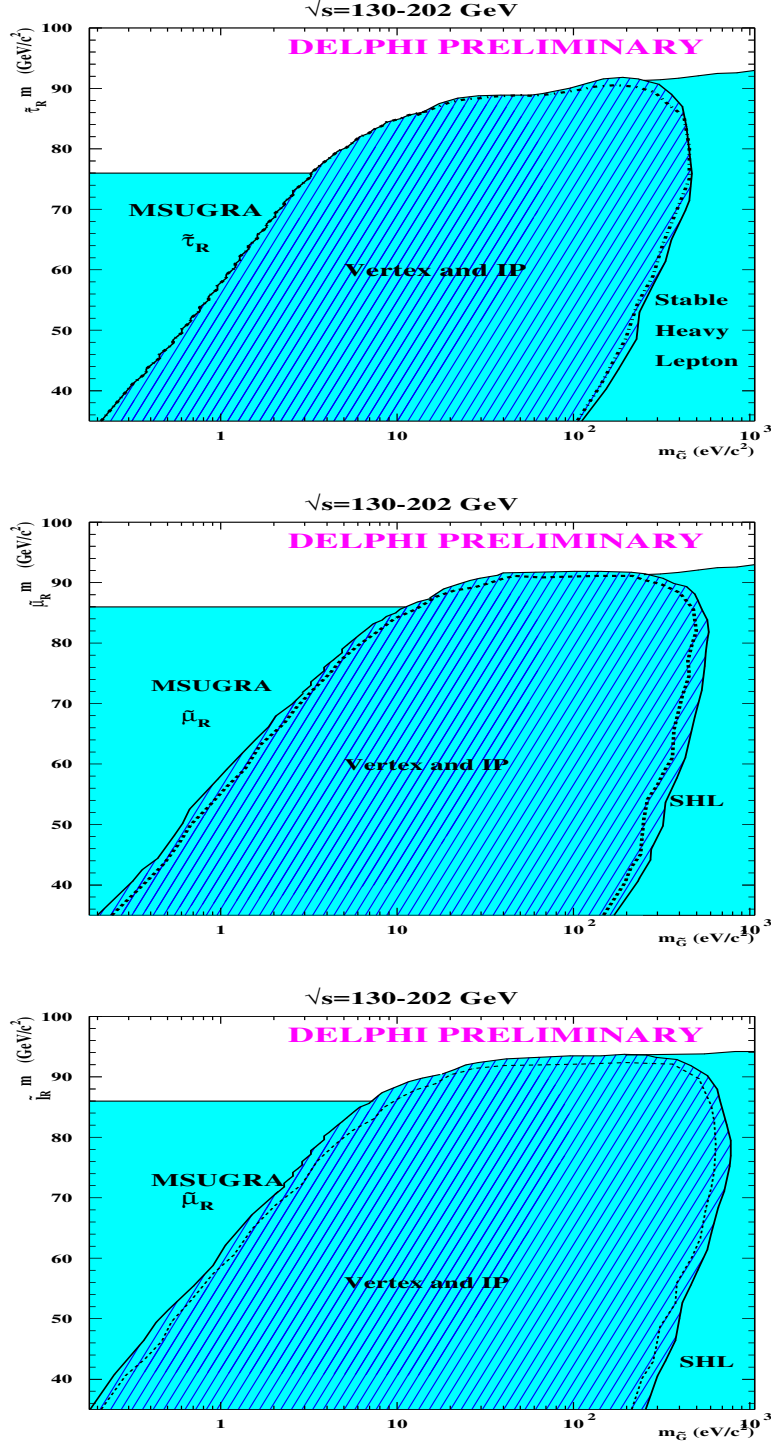
Figure 4: Exclusion regions in the $(m_{\tilde{G}}, m_{\tilde{\tau}_R})$ (a), $(m_{\tilde{G}}, m_{\tilde{\mu}_R})$ (b) and $(m_{\tilde{G}}, m_{\tilde{l}_R})$ (c) planes at 95% C.L. for the present analyses combined with the stable heavy lepton search and the search for $\tilde{\tau}_R$ in gravity mediated models, using all LEP2 data up to 202 GeV. The positive-slope hatched area shows the region excluded by the combination of the impact parameter and secondary vertex searches. The dashed line shows the expected limits.

14